

## Comparison of Machinability Performances in Milling of Al-7Si-Mg and Al-7Si-0.6Mg Alloys

Cem ALPARSLAN<sup>1</sup>, Şenol BAYRAKTAR<sup>1\*</sup>

<sup>1</sup>Department of Mechanical Engineering/ Faculty of Engineering and Architecture, Recep Tayyip Erdoğan University, TURKIYE

\*([senol.bayraktar@erdogan.edu.tr](mailto:senol.bayraktar@erdogan.edu.tr))

**Abstract** – In this study, the microstructural, mechanical and machinability properties of Al-7Si-Mg and Al-7Si-0.6Mg casting alloys were experimentally researched. While the microstructures of the alloys were determined by optical microscope, the hardness values were determined by Brinell method, elongation to fracture, yield (YS) and tensile strength (TS) values were measured by tensile tests. Milling experiments were performed 6 mm diameter of uncoated carbide end mill which two flutes in CNC vertical machining center using different cutting speeds ( $V$ ), feed rates ( $f$ ) and a constant depth of cut (DoC). In microstructural examinations, it was observed that the microstructure of the Al-7Si-Mg alloy comprised of  $\alpha$ -Al, primary Si, eutectic Al-Si,  $Mg_2Si$ ,  $\beta$ -Al(Fe, Mn)Si,  $\beta$ -Al<sub>5</sub>FeSi and  $\pi$ -AlSiMgFe phases. In addition to the existing phases,  $\beta$ -Al<sub>8</sub>Mg<sub>3</sub>FeSi<sub>6</sub> phase was formed in the microstructure of the Al-7Si-0.6Mg alloy. Al-7Si-0.6Mg alloy exhibited higher hardness, YS and TS and lower elongation to fracture (EF) values compared to Al-7Si-Mg alloy. In the milling tests, it was stated that the cutting force (CF), built-up layer (BUL) and built-up edge (BUE) reduced with the increment of the  $V$ , while it increased with the increment of the  $f$ .

**Keywords** – Al-Si-Mg Alloy, Microstructure, Mechanical Property, Machinability

### I. INTRODUCTION

Aluminum (Al) alloys are commonly used in many industrial areas due to their lightness, easy formability, high specific strength and corrosion resistance. Al is alloyed with different elements such as silicon (Si) and magnesium (Mg) because it cannot obtain the desired structural and mechanical features in its pure form. Al-Si based alloys have features such as low density and thermal expansion, easy castability, weldability and high thermal conductivity [1]. The addition of Mg in Al-Si alloys contributes to the improvement of the heat treatment properties as well as the high tensile and fatigue strength of the alloys. Due to these features, it is widely preferred in the production of engine blocks and cylinder heads in the automotive industry. In addition, it makes a significant contribution to low fuel economy by reducing the weight of vehicles and preventing air pollution. [2].

It is also used in aerospace, aerospace, electronics and other manufacturing industries for applications such as gearboxes, cylinder heads, fuel tanks, transmission covers, chassis and rims [7]. These alloys are usually produced by casting methods for low cost in mass production. Since the alloys produced by the casting method cannot be used directly in mechanical systems, machining operations are important so that these alloys can be used within precise and geometric tolerances after production. In order to obtain maximum efficiency from these alloys in mechanical systems, machinability properties should be known. When we look at the literature, it is seen that there are current studies on the structural, mechanical and machinability features of Al-Si alloys. In some studies on structural and mechanical features; Hekmat-Ardakan et al. stated that with the increment of Mg rate in A390 alloy, hard and

coarse primary Si particles were transformed into fine Mg<sub>2</sub>Si particles [8], Thirugnanam et al. the fracture behavior of the Al-7Si-Mg alloy depends upon the eutectic Si particles, the size and shape of the iron (Fe)-rich intermetallics [9], Taylor et al. found that YS of Al-7Si-Mg alloys increases linearly up to 0.6% wt Mg rate, but decreases at higher Mg ratios [10], Wu et al. showed that the YS and TS increased whereas the EF reduced with the increase of Mg content (0.3 and 0.6%) in the Al-Si-Mg alloy produced by the permanent mold casting (PMC) method [11], Yıldırım et al. determined that the TS and hardness of the alloy increased with the increment of the Mg ratio in the A356 aluminum alloy [12], Vench et al., Al-7Si-0.3Mg alloy exhibits high wear resistance due to Si content [13], Sha et al. determined that hardness and tensile strength values reached maximum values when high β” phase density occurred in Al-7Si-Mg alloy [14]. In some studies, on machinability properties; Dos Santos et al. found that increase the feed forces with increasing Si content in turning of Al-12Si and Al-16Si alloys [15], Bayraktar and Afyon reported that zinc (Zn-4%) and copper (Cu-3%) additions to the Al-7Si alloy decreased thrust force, torque, BUL and BUE formation in drilling with uncoated carbide drills and Cu additions showed better machinability properties [16]. Sharif et al. observed that the most significant factor affecting the machinability outputs in the drilling of A383 alloy was the feed rate parameter [17], Machado et al. reported that while turning of Al-(3%, 7 and 12)Si-0.6Mg alloy with TiN coated cemented carbide tools, cutting forces reduced with increment *V* and increased with increment *f* [18], Kisway et al. stated that BUE and abrasive wear mechanisms occurred in cutting tools when turning A356 alloy with uncoated and diamond-coated carbide inserts [19], Fernandes et al. found that plastic deformation, BUE and flank wear of the cutting tools occurred as a result of thread cutting with coated HSS (High speed steel) tools of AA6351 alloy [20], Kuczmaszewski et al observed that when milling (*V*:754 m/min, *f*: 0.15 mm/rev and DoC: 4 mm) Al10SiMg alloy with uncoated and TiB<sub>2</sub> and TiAlCN coated cutting tools, the best

machinability performance was obtained with TiAlCN coated cutting tools and BUE was formed in the cutting tools [21].

In this study, the microstructural and mechanical features of Al-7Si-Mg and Al-7Si-0.6Mg alloys manufactured by the PMC method were examined. In addition, the impacts of cutting parameters on CF, BUL and BUE formation in the milling of these alloys using different cutting parameters using uncoated carbide end mills were investigated comparatively.

## II. MATERIAL AND METHOD

Al-7Si-Mg and Al-7Si-0.6Mg alloys were melted in a medium frequency induction melting furnace and solidified by pouring into a permanent mold at room conditions at  $775 \pm 5$  °C. The samples obtained from the mold with the dimensions of 140x100x16 mm were machined to the dimensions of 70x50x15 mm using universal milling machine. Then, samples were prepared for machinability (Fig. 1a), mechanical (Fig. 1b and c), and microstructural tests (Fig. 1c).

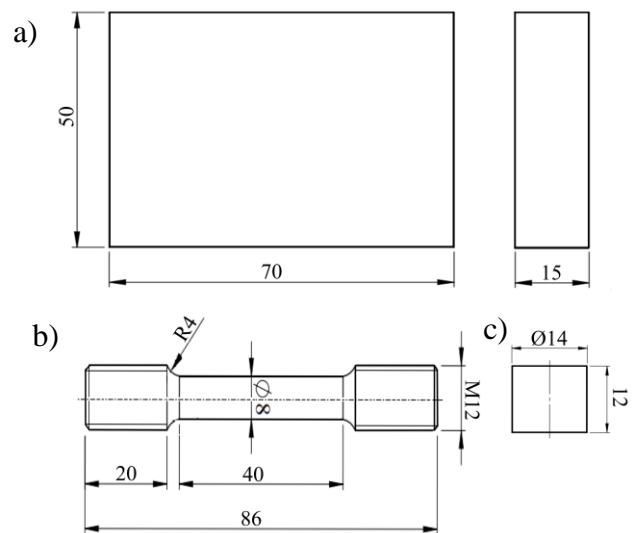


Figure 1. Technical drawings of samples, a) Machinability test sample, b) Tensile test sample and c) Microstructural and hardness test samples (Dimensions in mm)

These samples were prepared by standard metallographic methods (Bakelite-sanding-polishing) and their microstructures were examined under an optical microscope. Tensile specimens for mechanical tests were prepared in accordance with

ASTM E8 standard. In the tests, the elongation to fracture, tensile and yield strength values were measured using a fixed jaw of  $0.25 \text{ mm s}^{-1}$  and an average deformation rate of  $5.9 \times 10^{-3} \text{ s}^{-1}$ . In addition, the hardness of the alloy specimens were stated according to the Brinell hardness method using a  $62.5 \text{ kg}\times\text{f}$  load and a  $2.5 \text{ mm}$  diameter ball. Three samples were produced for each alloy in mechanical tests and the final test results were measured by taking the arithmetic mean of the values obtained from these samples.

Machinability tests were accomplished under dry cutting conditions in CNC vertical machining center using different  $V$  (50, 80 and  $110 \text{ m/min}$ ),  $f$  (0.08; 0.16 and  $0.24 \text{ mm/rev}$ ) and constant DoC ( $1 \text{ mm}$ ) parameters [22, 23]. Two flute uncoated carbide end mills with diameter of  $\text{Ø}6 \text{ mm}$  and  $30^\circ$  helix angle were used in the machinability tests. A total of eighteen experiments were performed according to the combination of cutting parameters and alloy material, using a new cutting tool for each experiment. The forces on the X, Y and Z axes were measured using the Kistler 5070A model dynamometer, amplifier and Dynoware software during the machinability tests (Fig. 2). The final cutting forces were calculated by taking the resultant of these forces for each test [24].

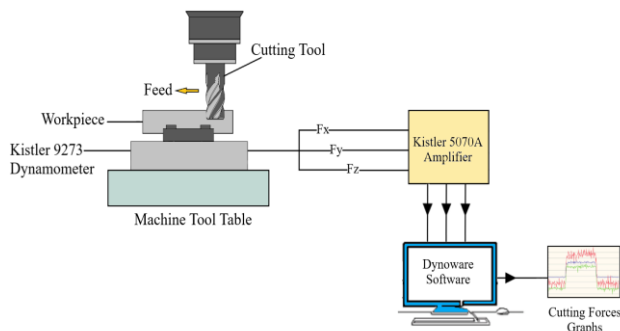


Figure 2. The schematic representation of the machinability test setup

### III. RESULTS

#### A. Microstructural Observations

It was observed that the microstructure of the Al-7Si-Mg alloy consists of Al-rich  $\alpha$ -Al, primary Si, eutectic Al-Si,  $\beta$ -Al<sub>5</sub>FeSi,  $\beta$ -Al(Fe,Mn)Si and  $\pi$ -Al-SiMgFe phases (Fig. 3a). In addition to Al-7Si-Mg alloy, AlFe-Si and  $\beta$ -Al<sub>8</sub>Mg<sub>3</sub>FeSi<sub>6</sub> phases

were sighted in the microstructure of the Al-7Si-0.6Mg alloy (Fig. 3b).

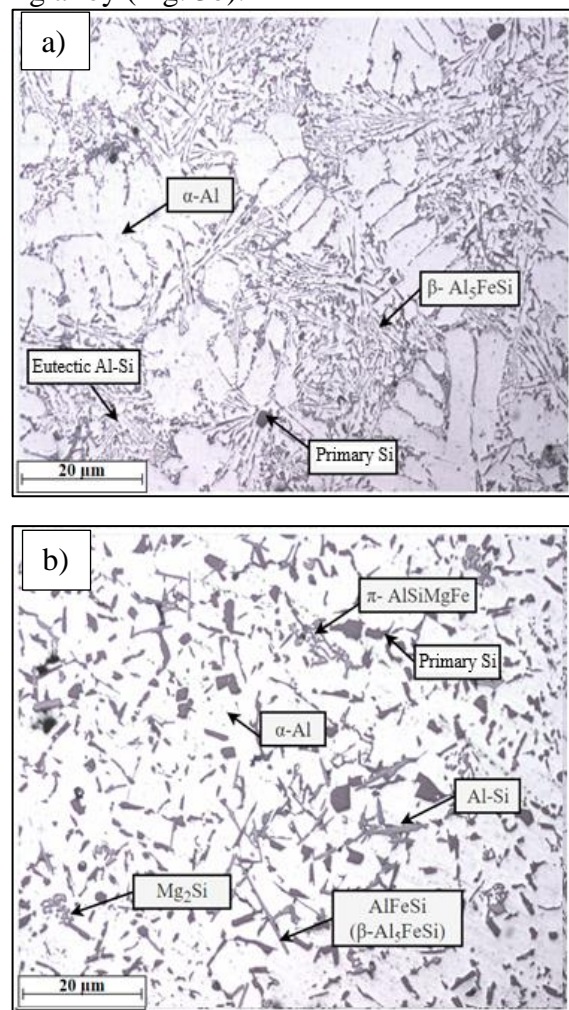
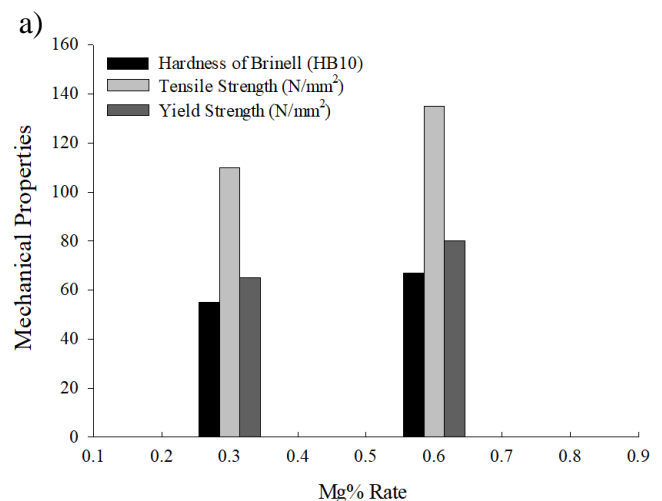


Figure 3. Microstructural photographs of alloys (10X), a) Al-7Si-Mg and b) Al-7Si-0.6Mg

#### B. Mechanical Properties

Hardness, elongation to fracture, yield and tensile strength values obtained from mechanical tests were given in Fig. 4a and b.



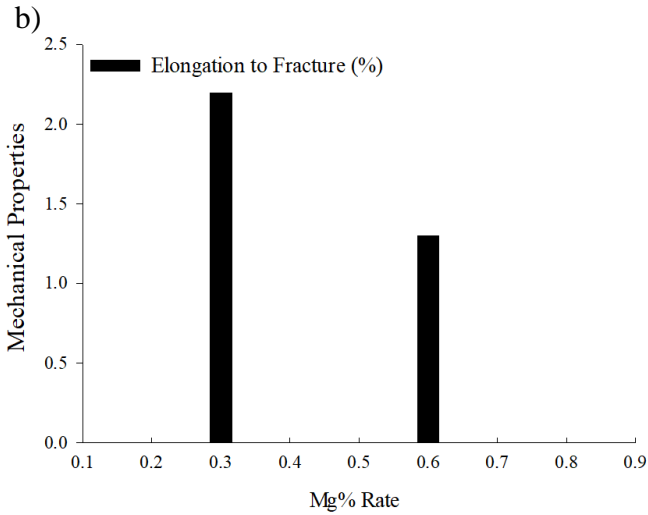


Figure 4. Mechanical features of Al-7Si-0.6Mg and Al-7Si-Mg alloys, a) Hardness, tensile and yield strenght values and b) Elongation to fracture value

In mechanical tests, the hardness, YS and TS values of the Al-7Si-0.6Mg alloy were found to be 21.82%, 22.73 and 23.08 higher, respectively, than the Al-7Si-Mg alloy, whereas the elongation to fracture values were found to be 40.91% lower.

### C. Machinability Properties

It was observed that the CF increased with the increment in  $f$  at constant  $V$  values in the milling of both alloys (Fig. 5). It was determined that the CF reduced with the increment in  $V$  at constant  $f$  (Fig. 6). The lowest CF was determined at  $V$  of 110 m/min and  $f$  of 0.08 mm/rev in Al-7Si-0.6Mg alloy.

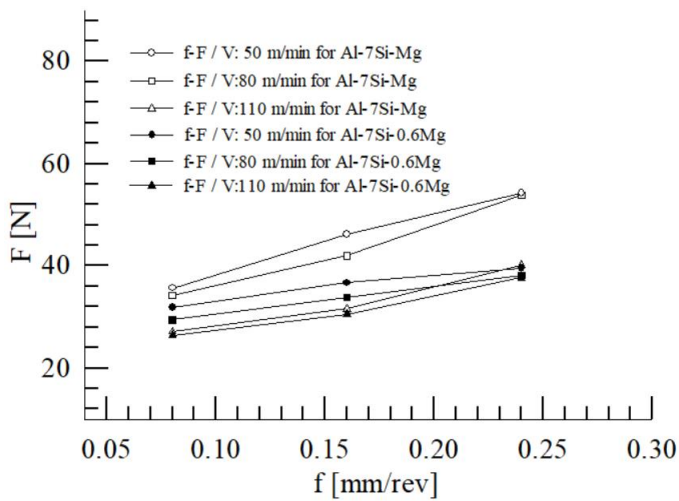


Figure 5. f-F relationship at constant cutting speed for Al-7Si-0.6Mg and Al-7Si-Mg alloys

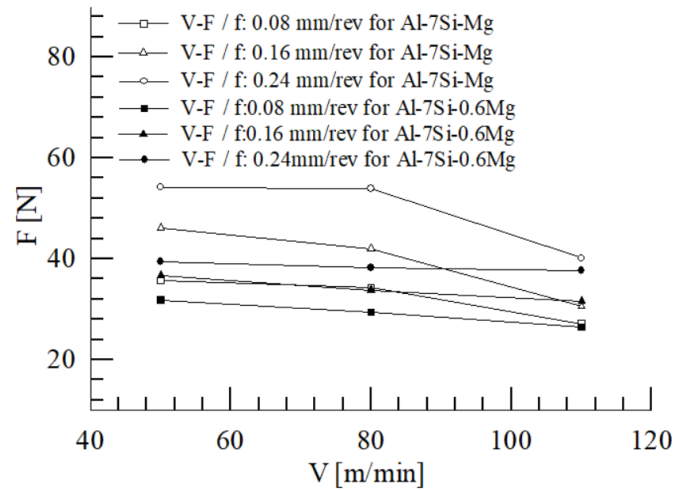


Figure 6. V-F relationship at constant feed rate for Al-7Si-0.6Mg and Al-7Si-Mg alloys

It was sighted that BUL and BUE were formed on the cutting edge of the cutting tool during the machining of each alloy. Minimum BUL and BUE formation were observed during machining of Al-7Si-0.6Mg alloy at  $V$  of 110 m/min and  $f$  of 0.08 mm/rev.



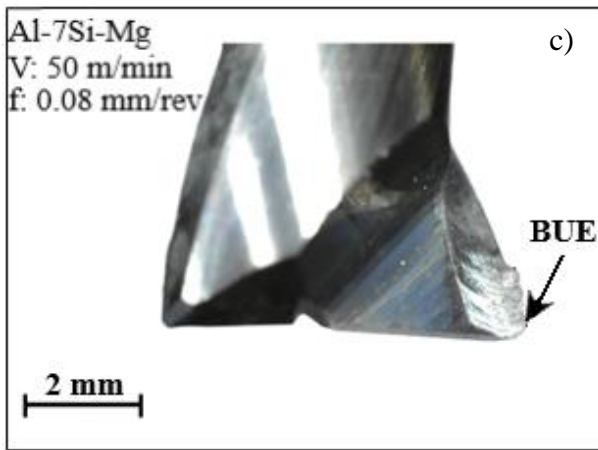


Figure 7. BUL and BUE formation on the cutting edge, a and b)  $V: 110 \text{ m/min}$ ,  $f: 0.08 \text{ mm/rev}$ ; c and d)  $V: 50 \text{ m/min}$ ,  $f: 0.08 \text{ mm/rev}$

#### IV. DISCUSSIONS

##### A. Microstructural Evaluations

As a result of the increase of  $\alpha$ -Al dendrites during the production of both alloys, Al-Si eutectic reaction took place in the microstructure. With the decrease in temperature depending upon time, Al, Si and  $\beta$ -Al<sub>5</sub>FeSi phases emerged and a triple eutectic reaction occurs. Then, the  $\beta$  phase partially transformed into the  $\pi$ -AlSiMgFe phase through a semi-peritectic reaction. In other words, the  $\pi$ -Fe phase with acicular morphology in the microstructure transformed into Fe-rich round intermetallics (Fig. 3b). A triple eutectic structure consisting of Al, Si and Mg<sub>2</sub>Si was formed [25]. The volume and amount of Fe-rich phases in the microstructure varied depending upon the Mg

content in the alloy. It was thought that needle-like  $\beta$ -Al<sub>5</sub>FeSi rich in Fe is dominant in alloys containing about 4% Mg by weight, and  $\beta$ -Al<sub>9</sub>Fe<sub>2</sub>Si<sub>2</sub> with Chinese-script morphology in alloys containing about 7% by weight of Mg [26].

##### B. Evaluation of Mechanical Properties

It was observed that while higher hardness, YS and TS values were measured in Al-7Si-0.6Mg alloy, lower EF was determined (Fig 4a and b). It was thought that this situation was caused by the formation and distribution of more precipitates due to the increment in the ratio of Mg in the  $\alpha$ -Al phase in the microstructure of the alloy. [2, 27].

##### C. Evaluation of Machinability Properties

In the machining of both alloys, it was determined that while the CF reduced with the increment of  $V$  at constant  $f$ , it increased with the increment of  $f$  at constant  $V$  (Fig. 5 and 6). The tool/chip interface temperature increased with the increment of  $V$ . Due to this temperature increment, the YS of the machined material reduced and the formation of plastic deformation became easier and the CF reduced [28, 29]. It was thought that the CF increased due to the increment in the  $f$  parameter and the increase in the volume of chip removed in unit time during cutting and the power required for plastic deformation [2].

It was observed that lower CF, BUL and BUE occurred in the milling of the Al-7Si-0.6Mg alloy compared to the Al-7Si-Mg alloy (Fig. 5-7). This was thought to be due to the formation of more Mg<sub>2</sub>Si precipitates in the microstructure of the Al-7Si-0.6Mg alloy and the decreased in EF depending on the increase in Mg content [2, 16] It was observed that the formation of BUL and BUE in cutting tools reduced with the increment in  $V$ . The tool/chip contact surface area decreased depending upon the increment in  $V$ . At the same time, high cutting temperatures occurred due to high  $V$  in Al-based alloys and plastic deformation of the chip was facilitated and BUL and BUE formation were reduced [29, 30]. It was observed that the formation of BUL and BUE in the cutting tool increased with the increment in  $f$ . It was thought that this situation was caused by the high volume of metal removal rate that caused high

pressure and CFs and the increase in the tool/chip interface contact area [31, 32].

## V. CONCLUSIONS

The results obtained from this study could be listed as follows.

1. Microstructure of Al-7Si-Mg alloy comprised of  $\alpha$ -Al, primary Si, eutectic Al-Si, Mg<sub>2</sub>Si,  $\beta$ -Al(Fe, Mn)Si,  $\beta$ -Al<sub>5</sub>FeSi and  $\pi$ -AlSiMgFe phases. It was sighted that  $\beta$ -Al<sub>8</sub>Mg<sub>3</sub>FeSi<sub>6</sub> phase was formed in addition to the existing phases in the microstructure of the Al-7Si-0.6Mg alloy.
2. Al-7Si-0.6Mg alloy exhibited higher hardness, YS and TS, whereas lower EF than Al-7Si-Mg alloy.
3. The cutting force, BUL and BUE formation reduced with the increment of the  $V$ , while it increased with the increment of the  $f$  in the machining of both alloys.
4. When machining Al-7Si-0.6Mg alloy under constant cutting conditions, lower CF, BUL and BUE were formed compared to Al-7Si-Mg alloy.

## REFERENCES

- [1] J. Grum, and M. Kisin, "Influence of microstructure on surface integrity in turning—part I: the influence of the size of the soft phase in a microstructure on surface-roughness formation," *International Journal of Machine Tools and Manufacture*, vol. 43(15), pp. 1535-1543, 2003.
- [2] Ş. Bayraktar, and O. Demir, "Processing of T6 heat-treated Al-12Si-0.6 Mg alloy," *Materials and Manufacturing Processes*, vol. 35(3), pp. 354-362, 2020.
- [3] S. Karagiannis, P. Stavropoulos, C. Ziogas, J. Kechagias, "Prediction of surface roughness magnitude in computer numerical controlled end milling processes using neural networks, by considering a set of influence parameters: an aluminium alloy 5083 case study," *Proceedings of the Institution of Mechanical Engineers, Part B: Journal of Engineering Manufacture*, vol. 228 (2), pp. 233-244, 2014.
- [4] R. S. Florea, K. N. Solanki, D.J. Bammann, J. C. Baird, J. B. Jordon, M. P. Castanier, "Resistance spot welding of 6061-T6 aluminum: Failure loads and deformation," *Materials and Design*, vol. 34, pp. 624–630, 2012.
- [5] R. Chen, Q. Xu, H. Guo, Z. Xia, Q. Wu, and B. Liu, "Correlation of solidification microstructure refining scale, Mg composition and heat treatment conditions with mechanical properties in Al-7Si-Mg cast aluminum alloys," *Material Science Engineering; A*, vol. 685, pp. 391–402, 2017.
- [6] D. Bakavos, and P. B. Prangnell, "Mechanisms of joint and microstructure formation in high power ultrasonic spot welding 6111 aluminium automotive sheet," *Materials Science and Engineering*, vol. 527, pp. 6320–6334, 2010.
- [7] M. Aamir, K. Giasin, M. Tolouei-Rad, and A. Vafadar, "A review: Drilling performance and hole quality of aluminium alloys for aerospace applications," *Journal of Materials Research and Technology*, vol. 9(6), pp. 12484-12500, 2020.
- [8] A. Hekmat-Ardakan, X. Liu, F. Ajersch, and X. G. Chen, "Wear behaviour of hypereutectic Al–Si–Cu–Mg casting alloys with variable Mg contents," *Wear*, vol. 269(9-10), pp. 684-692, 2010.
- [9] A. Thirugnanam, K. Sukumaran, U. T. S. Pillai, K. Raghukandan, and B. C. Pai, "Effect of Mg on the fracture characteristics of cast Al–7Si–Mg alloys," *Materials Science and Engineering: A*, vol. 445, pp. 405-414, 2007.
- [10] J. A. Taylor, D. H. John St, M. J. Couper, "Empirical analysis of trends in mechanical properties of T6 heat treated Al-Si-Mg casting alloys," *International Journal of Cast Metals Research*, vol. 12, pp. 419-430, 2020.
- [11] M. Z. Wu, J. W. Zhang, Y. B. Zhang, and H. Q. Wang, "Effects of Mg content on the fatigue strength and fracture behavior of Al-Si-Mg casting alloys," *Journal of Materials Engineering and Performance*, vol. 27(11), pp. 5992-6003, 2018.
- [12] M. Yıldırım, and S. Özyürek, "The effects of Mg amount on the microstructure and mechanical properties of Al–Si–Mg alloys," *Materials & Design*, vol. 51, pp. 767-774, 2013.
- [13] A. Vencl, I. Bobić, and Z. Mišković, "Effect of thixocasting and heat treatment on the tribological properties of hypoeutectic Al–Si alloy," *Wear*, vol. 264(7-8), pp. 616-623, 2008.
- [14] G. Sha, H. Möller, W. E. Stumpf, J. H. Xia, G. Govender, S. P. Ringer, "Solute nano structures and their strengthening effects in Al–7Si–0.6Mg alloy F357," *Acta Materialia*, vol. 60, pp. 692-701, 2012.
- [15] G. R. Dos Santos, D. D. Da Costa, F. L. Amorim, and R. D. Torres, "Characterization of DLC thin film and evaluation of machining forces using coated inserts in turning of Al–Si alloys," *Surface and Coatings Technology*, vol. 202(4-7), pp. 1029-1033, 2007.
- [16] Ş. Bayraktar, and D. Afyon, "Machinability properties of Al–7Si, Al–7Si–4Zn and Al–7Si–4Zn–3Cu alloys," *Journal of the Brazilian Society of Mechanical Sciences and Engineering*, vol. 42(4), pp. 1-12, 2020.
- [17] A. Sharif, and S. Idris, "Performance and wear mechanisms of uncoated, TiAlN, and AlTiN-coated carbide tools in high-speed drilling of Al-Si alloy," *The International Journal of Advanced Manufacturing Technology*, vol.113(9), pp. 2671- 2684. 2021.
- [18] P. A. B. Machado, J. M. do Vale Quaresma, A. Garcia, and C. A. dos Santos, "Investigation on machinability in turning of as-cast and T6 heat-treated Al-(3, 7, 12%) Si-0.6% Mg alloys," *Journal of Manufacturing Processes*, vol. 75, pp. 514-526, 2022.
- [19] H. A. Kishawy, M. Dumitrescu, E. G. Ng, and M. A. Elbestawi, "Effect of coolant strategy on tool

- performance, chip morphology and surface quality during high-speed machining of A356 aluminum alloy," *International Journal of Machine Tools and Manufacture*, vol. 45(2), pp. 219-227, 2005.
- [20] G. H. Fernandes, G. H. Lopes, L.M. Barbosa, P. S. Martins, and A. R. Machado, A R, "Wear mechanisms of diamond-like carbon coated tools in tapping of AA6351 T6 aluminium alloy," *Procedia Manufacturing*, vol. 53, pp. 293-298, 2021.
- [21] J. Kuczmaszewski, P. Pieško, & M. Zawada-Michałowska, "Carbide milling cutter blades durability during machining of Al-Si casting alloy," *Multidisciplinary Aspects of Production Engineering*, vol. 1(1), pp. 169-175, 2018.
- [22] T. O. Sadiq, B. A. Hameed, J. Idris, O. Olaoye, S. Nursyaza, Z. H. Samsudin, and M. I. Hasnan, "Effect of different machining parameters on surface roughness of aluminium alloys based on Si and Mg content," *Journal of the Brazilian Society of Mechanical Sciences and Engineering*, vol. 41(10), pp. 1-11, 2019.
- [23] G. M. Uddin, F. M. Joyia, M. Ghufran, S. A. Khan, M. A. Raza, M. Faisal, S. M. Arafat, S. W. H. Zubair, M. Jawad, M. Q. Zafar, M. Irfan, B. Waseem, I. A. Chaudhry, and I. Zeid, "Comparative performance analysis of cemented carbide, TiN, TiAlN, and PCD coated inserts in dry machining of Al 2024 alloy," *The International Journal of Advanced Manufacturing Technology*, vol. 112, pp. 1461-1481, 2021.
- [24] A. P. Hekimoğlu, Ş. Bayraktar, & Y. Turgut, "Kesme Hızı ve İlerlemenin Al-35Zn Alaşımının İşlenebilirliğine Etkisinin İncelenmesi". In 2nd International Symposium on Innovative Approaches in Scientific Studies pp. 77-83, 2018.
- [25] X. Wu, H. Zhang, Z. Ma, T. Tao, J. Gui, J. Song, W. and Zhang, H, "Interactions between Fe-rich intermetallics and Mg-Si phase in Al-7Si-xMg alloys," *Journal of Alloys and Compounds*, vol. 786, pp. 205-214, 2019.
- [26] S. Jana, R. S. Mishra, J. B. Baumann, and G. Grant, "Effect of friction stir processing on fatigue behavior of an investment cast Al-7Si-0.6 Mg alloy," *Acta Materialia*, vol. 58(3), pp. 989-1003, 2010.
- [27] M. Z. Wu, J. W. Zhang, Y. B. Zhang, and H. Q. Wang, "Effects of Mg content on the fatigue strength and fracture behavior of Al-Si-Mg casting alloys," *Journal of Materials Engineering and Performance*, vol. 27, pp. 5992-6003, 2018.
- [28] P. A. B. Machado, J. M. do Vale Quaresma, A. Garcia, and C. A. dos Santos, "Investigation on machinability in turning of as-cast and T6 heat-treated Al-(3, 7, 12%) Si-0.6% Mg alloys," *Journal of Manufacturing Processes*, vol. 75, pp. 514-526, 2022.
- [29] Ş. Bayraktar, Ç. Çamkerten, and N. Salihoğlu, "Bakır ve Silisyum İhavelerinin Al-25Zn Alaşımının CVD Al<sub>2</sub>O<sub>3</sub> Kaplamalı Takımlarla Tornalanmasında İşlenebilirliğe Etkisinin İncelenmesi," *Gazi University Journal of Science Part C: Design and Technology*, vol. 8 (1), pp. 79-93, 2020.
- [30] A. Acır, Y. Turgut, M. Übeyli, M. Günay, and U. Şeker, "A study on the cutting force in milling of boron carbide particle reinforced aluminium composite," *Science and Engineering of Composite Materials*, vol. 16(3), pp. 187-196, 2009.
- [31] M. Tash, F. H. Samuel, F. Mucciardi, H. W. Doty, and S. Valtierra, "Effect of metallurgical parameters on the machinability of heat-treated 356 and 319 aluminum alloys," *Materials Science and Engineering: A*, vol. 434 (1-2), pp. 207-217, 2006.
- [32] M. S. Najiha, M. M. Rahman, and K. Kadirgama, "Experimental investigation and optimization of minimum quantity lubrication for machining of AA6061-T6," *International Journal of Automotive and Mechanical Engineering*, vol. 11, pp. 2722, 2015.